

Green synthesis of Cu₂O hollow microspheres

Abhishek K. Bhardwaj^{1*}, Abhishek Shukla², S. C. Singh², Kailash N. Uttam²,
Gopal Nath³, Ram Gopal^{2*}

¹Center for Environmental Science, Department of Botany, University of Allahabad, Allahabad 211002, India

²Laser Spectroscopy and Nanomaterials Lab, Department of Physics, University of Allahabad, Allahabad 211002, India

³Department of Microbiology, Institute of Medical Science, Banaras Hindu University Varanasi, 221005, India

*Corresponding author, Tel: (91) 5322460993; E-mail: profrgopal@gmail.com, bhardwajak87@gmail.com

Received: 31 March 2016, Revised: 10 August 2016 and Accepted: 21 December 2016

DOI: 10.5185/amp.2017/215

www.vbripress.com/amp

Abstract

Green synthesis of nanoparticles (NPs) from biological constituents extracts have emerged as potential methods for the fabrication of metallic NPs. In the present study, Cuprous oxides hollow microspheres (Cu₂O-HMs) have been synthesized using *D. carota* pulp waste extract (CPWE). This Cu₂O hollow microsphere (Cu₂O-HMs) synthesis is environmental friendly, at room temperature. The aqueous copper ions are reduced into Cu₂O-NPs, when these ions interact with active reducing constituents of CPWE and very little amount of sodium hydroxide for enhancing rate of reaction. The Cu₂O-NPs have been characterized by UV-Vis spectroscopy, Fourier transform infrared spectroscopy (FTIR), X-ray diffraction (XRD), and Transmission electron microscopy (TEM). XRD measurements contain average size of Cu₂O-NPs are approx 12 nm which is responsible to form Cu₂O-HMs. UV-VIS spectra show that the surface Plasmon resonance peak of copper is observed at 490 nm. FTIR measurements indicate the presence of different reducing constituents in *D. carota* extract which is responsible for reducing and capping bioreduced Cu₂O-HMs. TEM measurement shows that most Cu₂O-HMs are spherical in shape and are responsible to form microsphere and nanotubes. Antibacterial activity of Cu₂O-HMs tested on *S. aureus* shows a comparable zone of inhibition. These interesting results may be applicable for the cost-effective, environmental friendly, surface disinfectant and biomedical fields. Copyright © 2017 VBRI Press.

Keywords: Pulp waste extract, Cu₂O-HMs, green synthesis, biosynthesis, *D. carota*.

Introduction

Metal nanoparticles (NPs) have attracted considerable attention from past decades, due to their unique chemical and physical properties such as tunable Surface Plasmon Resonance (SPR) and their potent application in biomedical science [1-3], in gas sensing [4], CO oxidation [5], Photo catalysis [6-10], and photochemical evolution of H₂ from water [11], organic synthesis [12], and photocurrent generation [13, 14]. Cuprous oxide nanoparticles (Cu₂O-NPs) is an important metal-oxide p-type semiconductor with a direct small band gap of 2.17 eV [15], which makes it a promising material for the conversion of solar energy into electrical or chemical energy. Cu₂O nanostructure has been demonstrated to possess properties useful for applications Cu₂O-NPs have been prepared by several different methods, such as wet chemical reduction [16], electro deposition [17-19], sonochemical method [20], thermal relaxation [21], liquid phase reduction [22] vacuum evaporation [23] and Pulse Laser Ablation (PLA) [24, 25] because of the diversity and importance of variable applications. In the wet chemical reduction method metal ion converts into zerovalent metal. In this method reported some organic

chemicals (reducing agent) such as sodium borohydrate, sodium hypophosphite or hydroxylamine hydrochloride, potassium bitartrate, formaldehyde, dimethyl formaldehyde, hydrazine, etc. which are harmful for environment and biological creatures. In recent scenario scientist focused on the green chemistry which deals the design of chemical processes and product that reduce or minimize the use and generation of hazardous substances [26, 27].

Carrots have been known to be good sources of natural antioxidants including carotenoids, vitamins, phenolic compounds and flavonoids. Carrot pulp and residue from the processing of different fruits and vegetables are traditionally considered as an environmental problem, are being increasingly recognized as sources for obtaining high phenolic products [28]. Due to large population of India, large amount of garbage waste is produced which need to maximum and sustainable utilization of resources. Here carrot pulp waste has been used for the synthesis of Cu₂O-HMs, which is generally discarded off in environment. These phenolics compounds may be boon for inexpensive, large scale and eco-friendly synthesis of metal NPs. [29]. Previous studies have been indicated that Cu₂O-NPs have antimicrobial activity against *E. coli* and

S. coccus species [30], and similar antifungal properties were also reported [31].

The easy availability of copper, and having related properties like of other expensive noble metals, such as silver and gold, has made it a better choice to work. In this work not only simple environmental friendly and cost-effective synthesis of Cu_2O microsphere but other hand utilization of garbage waste product. Several constituents of CPWE, including sugars, proteins, terpenoids, polyphenols, alkaloids, and phenolic acids, play a significant role for bioreduction of metal ions and surface functionalization, and this results the formation of Cu_2O -HMs. This way a new approach is open to synthesis nonmaterial without using any polymer dispersant and other harmful reducing agents. Bactericidal activity has been performed against *S. aureus* using Cu_2O -NPs.

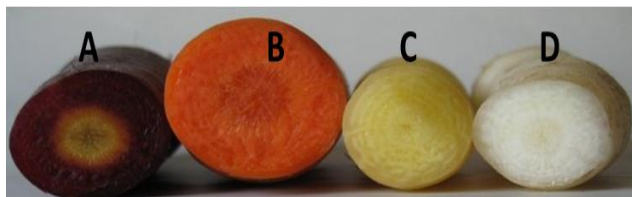


Fig. 1. Different color of carrot shows (A) purple (B) orange (C) yellow and (D) white carrot from www.carrot museum.com.

Experimental

Materials

Analytical grade copper sulfate pentahydrate ($\text{CuSO}_4 \cdot 5\text{H}_2\text{O}$, 99.8%, pure), sodium hydroxide (NaOH, 99.0% pure) and distilled water were supplied by Merck (India). Chemicals required for nutrient agar and nutrient broth were purchased from HiMedia Laboratories Pvt. Ltd. Mumbai, India and carrot obtained from market of Allahabad India.

Methods

Preparation of carrot pulp waste extract

The fresh orange carrot root (*Daucus carota L.*) collected from Allahabad market was extensively washed three times with distilled water and air dried. The carrot was crushed in juicer and carrot pulp waste was collected. This carrot pulp was dried at 40°C for 24 hours and finely it has stored in an air tied container. About 15 g powdered carrot pulp waste was transferred into 200 ml beaker containing 100 ml double distilled water, mixed well using magnetic stirrer at 40°C for half an hour extract was filtered (0.45μ) and was used as a reducing as well as stabilizing agent for synthesis of Cu_2O -NPs.

Synthesis of Cu_2O -HMs

Synthesis of colloidal Cu_2O HMs has been done in following steps; 100 ml of carrot pulp extract was mixed into 100 ml of 0.01M aqueous solution of $\text{CuSO}_4 \cdot 5\text{H}_2\text{O}$ magnetic stirrer for 10 min. The mixture solution was turned out to be green. The greenish supernatant was

separated and 100 ml of supernatant was added drop wise drop at the rate of 5 ml/3 minute into 100 ml of $0.2 \mu\text{M}$ aqueous NaOH using burette, with continuous stirring at 40 - 60°C . Within an hour, greenish color of solution turned into dark yellow precipitate form. Precipitate was separated and washed by double distilled water using centrifuge 4000 rpm. Collected precipitate (Cu_2O HMs) was dried in oven at 50°C for 8 hrs and used for characterization.



Fig. 2. It is a reaction, (A) illustrate $\text{CuSO}_4 \cdot 5\text{H}_2\text{O}$ (B) Carrot waste extract (C) Mix up A and B and (D) Cu_2O HMs after reduction.

Possible mechanism synthesis of Cu_2O -HMs

As we know plant metabolites such as terpenoids, polyphenols, sugars, alkaloids, phenolic acids, and proteins, play an important role in the bioreduction of metal ions and capping agent [32]. Carrot is orange color because of the rich source of carotene which may responsible for capping agent or reaction stabilizer Fig. 1. The Cu_2O -HMs may formation of extract containing different phenolics species such as terpinoid; (eugenol), amino acid (tyrosine, tryptophan), flavonoid (luteonine, quercetin), and Vitamins (β -carotene, ascorbic acid and tocopherol) are possible. FTIR support presence of L-ascorbic acid or vitamin-c acid in CPE which play a significant role in reduction of copper ions [33, 34]. Xiang reported that ascorbic acid has high water solubility and strong polarity. L-Ascorbic acid behaves as a vinyllogous carboxylic acid in which the electrons in the double bond, hydroxyl group lone pair, and the lactone ring carbonyl double bond form a conjugated system. The charge transfer induced molecular changes in ascorbic to semidehydroascorbic acid and dehydroascorbic acid during reduction of the Cu^{2+} to Cu^0 have been shown Fig. 3(a). The possible charge transfer enable releasing two electrons which are responsible to take part in the reduction of Cu^{2+} to Cu^0 . Mechanism of stability of Cu_2O -NPs can be explained from two aspects shown Fig. 3(b). First one is the reduction and second one is the capping effect of phenolic compounds of CPWE. The lone pair electrons in the polar groups of L-ascorbic acid/phenolic compounds can occupy two sp orbitals of the copper ion to form a complex compound. The reduced copper is thus capped with phenolic compounds and synthesizes Cu^0 -NPs through reduction of Cu^{2+} inside the nanoscopic templates. But in this case low concentration of phenolic acid and other reducing/capping agent and also dissolve

oxygen in system interact with Cu^0 form Cu_2O -HMs and further formation of microsphere. Phenolic group containing $-\text{OH}$ groups as a reducing and capping agent in aqueous solution **Fig. 3** shows this is responsible for reduction of Cu^{++} to Cu^+ and Cu^0 and HMs capping with biomolecules simultaneously. After consumption of a $-\text{OH}$ group Cu^{2+} convert Cu^+ may responsible for green color because in case of copper 3d orbital has greater tendency to get electron. Cu^+ has less electron affinity than Cu^{++} so need strong reducing agent (NaOH) for complete reduction and finally convert into Cu^0 and further oxidized in form of Cu_2O -NPs due to oxygen present in the synthesizing medium.

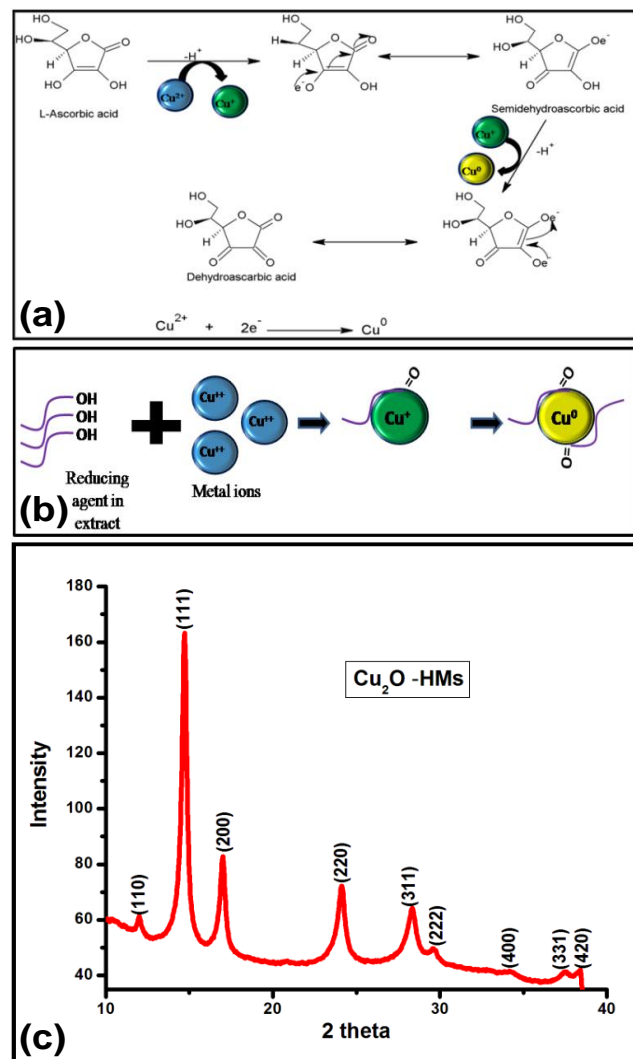


Fig. 3. (a) A plausible schematic illustration of reduction of Cu^{++} to Cu^0 by ascorbic acid and conversion of ascorbic acid into dehydroascorbic acid (b) reducing and capping process (c) XRD pattern of the powder sample of Cu_2O -HMs.

Characterization of synthesized Cu_2O -HMs

In order to determine the crystal structure of the Cu_2O -HMs mediated with carrot pulp waste extract and to measure the purity of the synthesized Cu_2O -HMs the powder X-ray diffraction analysis was performed. The XRD pattern of dry Cu_2O -HMs powder was recorded

using Indus-2, beamline-21 synchrotron radiation source having wavelength 0.6255\AA . The maximum surface plasmon resonance (SPR) of the green synthesized Cu_2O -HMs solution was monitored by UV-VIS absorption spectra of synthesized colloidal solutions of HMs using Perkin Elmer Lambda 35, double beam spectrophotometer in the range from 300 to 800 nm with a resolution of 0.5 nm. To investigate the surface modification properties of synthesized Cu_2O -HMs, IR spectrum was recorded on Bomem ATR-Fourier transform infrared spectrometer in the range $480\text{--}4000\text{ cm}^{-1}$ with a resolution of 4 cm^{-1} . The study confirms the formation and stabilization of Cu_2O -HMs in the aqueous medium using biological molecules. The measurements were made as a function of reaction time at room temperature. High resolution transmission electron microscope Tecnai G2-20 (FEI company, Netherland) operated at 200 kV was used to determine the particle size and shape of the synthesized Cu_2O -HMs. Samples for TEM images were prepared as colloidal Cu_2O -HMs sonicated using ultrasonic bath and by placing a drop of sonicated copper solution on a carbon coated grid 300 mesh and it was allowed to dry in oven for TEM image, scanning electron microscopy (SEM, JEOL JXA-1800 electron probe microanalyser) operating at 15 kV was used for looking surface morphology. Zone of inhibition were tested using Kirby-Bauer well diffusion method [3]. The concentration of bacteria inoculants was 5×10^6 colony forming unit (CFU)/ml used and incubate at 37°C for 24 hrs, after adding Cu_2O in well of nutrient agar. Bacterial growth curve was determined using UV-VIS spectrophotometer (Perkin Elmer Lambda 35). Nutrient broths containing 5×10^6 CFU of bacteria/ml in the growth phase were used. The data were recorded at 0 min to 24 hrs continuous and last data were recorded after completing 48 hrs of experiment for both the cases with and without mixing of Cu_2O -HMs.

Results and discussion

Powder X-ray diffraction analysis

Powder X-ray diffraction (XRD) patterns was observed in the 2θ range $10\text{--}40^\circ$ of the as-prepared hollow microsphere as shown in **Fig. 3(c)**. The peak positions with 2θ values of 11.888° , 14.578° , 16.874° , 23.907° , 28.128° , 29.387° , 34.076° , 37.241° , and 38.241° are indexed as interplanar distances calculated for (110), (111), (200), (220), (311), and (222), (400), (331), and (420) from XRD patterns match from the International Center of Diffraction Data card (JCPDS file no. 05-0667) confirming the formation of a cubic phase Cu_2O with a cuprite structure. No other diffraction peaks arising from metal Cu or CuO appear in the XRD patterns are observed in agreement with the earlier workers [35]. The particle size was calculated from XRD peaks using Debye Scherrer's formula,

$$D = \frac{K\lambda}{\beta \cos\theta}$$

where, the constant $K = 0.97$, $\lambda = 0.6255 \text{ \AA}$ is the wavelength of X-ray line used and β is the full width at half maximum. The crystalline size of Cu_2O HMs calculated from the XRD peaks is approx. 12 nm.

UV-vi spectra analysis of Cu_2O -HMs

The yellowish color powder of Cu_2O -HMs was dispersed in double distilled water for characterization by UV-Vis spectrophotometer. The SPR peak at 490 nm of Cu_2O shows collective oscillations of conduction electrons at the surface of nanosized particles absorb visible electromagnetic waves responsible to confirmation of nanoscale Cu_2O particles [36]. The collective oscillations are due to: (a) acceleration of the conduction electrons by the electric field of incident radiation, (b) presence of restoring forces that result from the induced polarization in both the particle and surrounding medium and (c) confinement of the electrons to dimensions smaller than the wavelength of light. The different color of spectra reveals how reaction takes place. In the present study, the CPWE-mediated synthesis of Cu_2O -HMs was investigated by UV-VIS spectroscopy which suggests conversion of Cu^{++} to Cu^0 . Four different spectra have been recorded such as CPWE, copper sulfate, copper sulfate plus CPWE and pure Cu_2O in DW shown in Fig. 4(a) which are visualized in A, B, C, and D respectively of Fig. 2. This is visibly detected by characteristic colour change of the reaction mixtures due

to presence of reducing agent such as ascorbic acid, phenolics and carotenoid compounds of carrot are capable of reducing the ions [37].

The optical band gap of synthesized Cu_2O microspheres was estimated by employing absorption data, the absorption coefficient, α , of the microsphere solution of Cu_2O -HMs under the Beer's law, is related to its band gap energy by $\alpha = A (h\nu - E_g)^n/h\nu$, where A is a constant, E_g is the band gap of material, and the exponent n may have the values $1/2$, 2 , $3/2$, and 3 corresponding to allowed direct, allowed indirect, forbidden direct, and forbidden indirect semiconductor, respectively [38]. The region of fundamental absorption, which corresponds to the electronic transition from top of the valance band to the bottom of conduction band, can be utilized to determine the band gap energy of the material using above relation. The $h\nu$ derivative of $\ln(\alpha h\nu) = n \ln A (h\nu - E_g)$ makes following expression

$$\frac{d\{\ln(\alpha h\nu)\}}{d(h\nu)} = \frac{n}{(h\nu - E_g)}$$

The plot of $d\{\ln(\alpha h\nu)\}/d(h\nu)$ versus $h\nu$ shows a divergence at energy equal to the band gap E_g , corresponding to the electronic transition as displayed in Fig. 4(c). This plot suffers comparatively less error in the band gap determination as compared to the Tauc plot. Band gap of the Cu_2O microsphere obtained by bio-reduced copper ion has band gap energy of 2.35 eV. Fig. 4(b&c) shows band gap of synthesized microspheres.

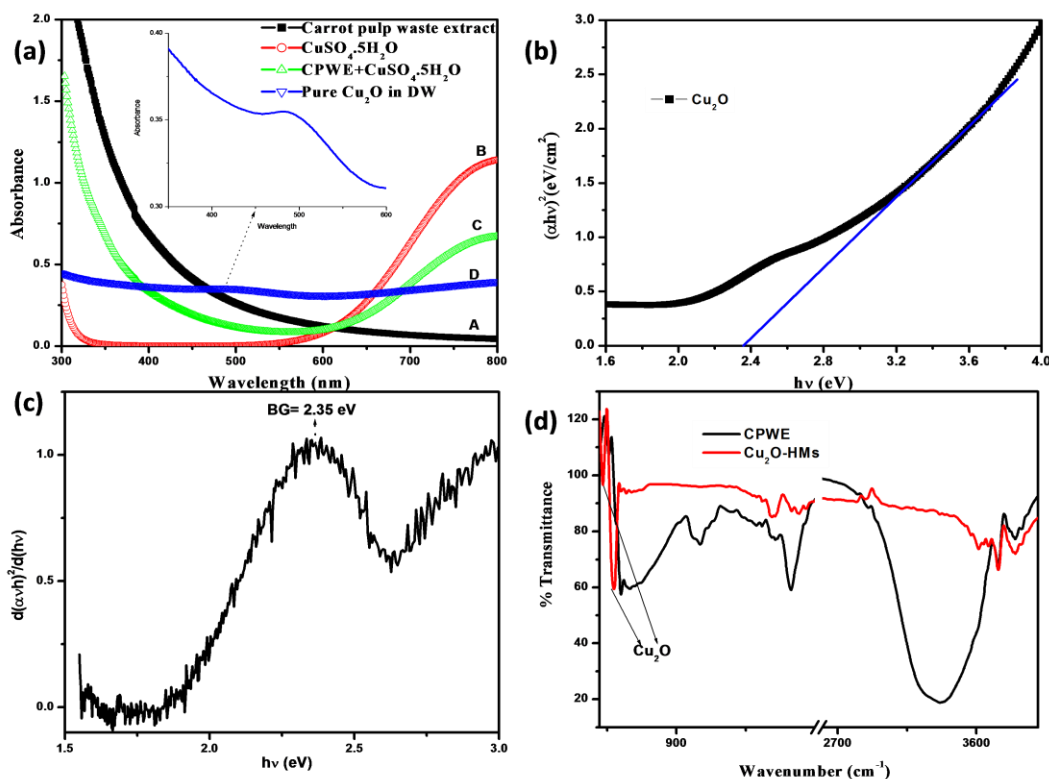


Fig. 4. (a) Recorded UV-VIS absorption spectrum of synthesized Cu_2O -HMs, (b&c) Tauc plot for the synthesized colloidal oxide of Cu_2O -HMs, and (d) recorded ATR-FTIR spectra of the synthesized Cu_2O -HMs.

ATR FTIR spectra analysis

The ATR-FTIR spectra of powder of Cu₂O-HMs have been recorded in region 480-4000 cm⁻¹. The three characteristic bands observed at wavenumber 432, 497 and 613 cm⁻¹ are assigned to the Au mode, Bu mode, and other Bu mode of CuO [39]. The IR absorption peak at around wave number 430 and 613 cm⁻¹ can be attributed to the lattice vibration of the Cu₂O and wave number 559, 1047, 1215, 1639, 1736 cm⁻¹ show the surface of Cu₂O NPs make up by different group present like alkyl halide, C-N, C-H, N-H, C=O respectively. The peak positions assigned to 557, 613, 1047, 1215, 1639 and 1736 cm⁻¹ suggest reduction and surface modification via different bio-molecules such as ascorbic acid, alcohols, aldehydes, ketones and carboxylic acid.

Surface morphology analysis

The TEM images of the as-prepared Cu₂O hollow microspheres are shown in Fig. 5 (a&b). It is clearly observable microsphere made up of smaller particles, size less than 20 nm.

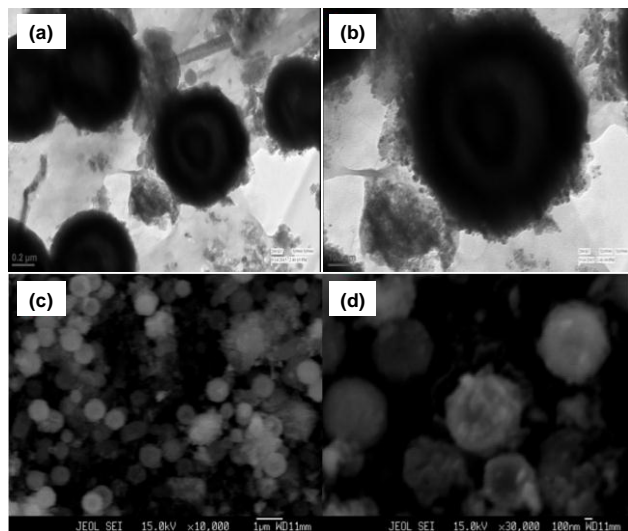


Fig. 5. (a, b) HRTEM image of synthesized Cu₂O hollow microsphere and (c, d) SEM micrograph image of synthesized Cu₂O-HMS hollow microsphere.

The morphology of the sample has been identified as rough, porous, hollow microsphere structures by TEM and SEM. Some fold and channels also appear which have smaller width 20 to 50 nm. Most of the microspheres are uniform, and the diameter ranges from 650 nm to 800 nm. In the SEM image clearly appear Fig. 5(c&d) some unclosed sphere which contain smaller sphere approx 50-100 nm. Several researcher prepared Cu₂O-HMs [10, 40] but this one of the best cost effective synthesis method.

Bacterial susceptibility studies

Antibacterial test of synthesized Cu₂O -HMs was done on *Staphylococcus aureus* (ATCC 25323) as a gram positive bacteria using Kirby-Bauer well diffusion method. The significant zone of inhibition diameter ~8 mm and 12 mm

were observed unheated Cu₂O and heated (200°C for 24 hr) Cu₂O respectively in Fig. 6(a) against *S. aureus*. Cell wall of Gram positive bacteria composed of a thick peptidoglycan layer, consisting of linear polysaccharide chains cross linked by short peptides, thus forming more rigid structure leading to difficult penetration of the greater size NPs, while in Gram negative bacteria the cell wall possesses thinner peptidoglycan layer [3]. In all the experiments adequate aseptic measures were taken. For the well diffusion method, 100 µl of *S. aureus* suspension of about 5 x 10⁶ CFU ml⁻¹ was spread over Mueller-Hinton agar plates using sterilized cotton swabs and 20 µl Cu₂O-HMs placed on the bacterial lawns. The solutions gradually diffused into the neighboring bacterial lawns and the area around the discs depleted of bacterial population was regarded as a measure of the antibacterial property of the powder.

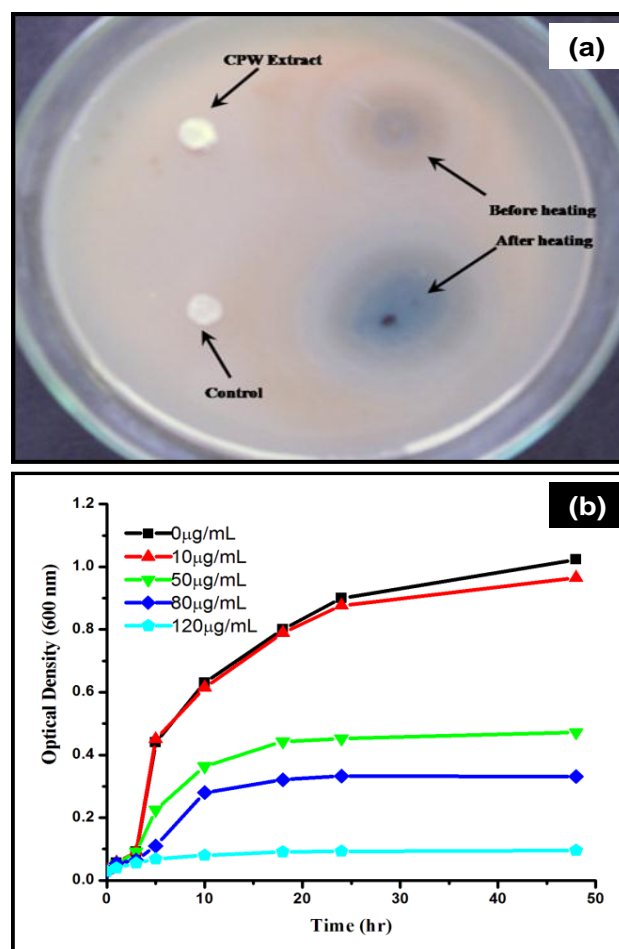


Fig. 6. (a) Zone of inhibition of Cu₂O microsphere, Cu₂O heated microsphere, CPWE and control against *S. aureus* bacteria and (b) the optical density (at 600 nm) growth curve at different time interval with 0, 10, 50, 80, 110 µg/ml of Cu₂O doses against *S. aureus* bacteria.

Bacterial growth curve

To confirm the results obtained, we further extended the study in LB media (dynamic growth) to see how it affects the growth rate of *S. aureus* in a liquid culture media. It is known that the amount of bacterial colonies in the media

is proportional to the optical density (OD) of the media containing the bacteria. So, by observing the OD (or the amount of light absorbed at 600 nm), the growth rate of *S. aureus* under the influence of Cu₂O-HMs can be measured. **Fig. 6(b)** shows the growth curve of *S. aureus* at different time intervals with different concentrations of Cu₂O-HMs.

The reduction is more prominent for higher doses of Cu₂O-HMs. The quantitative investigation of the antimicrobial activity of Cu₂O-HMs has been done by supplementing 10, 50, 80 and 110 µg/L of Cu₂O-HMs in cultured *S. aureus* colonies on LB broth (5 x 10⁶ colony forming unit's ml⁻¹). The broths were incubated for 50 hrs at 37 °C. The result clearly shows the antibacterial properties of Cu₂O-HMs. The characteristics log phase is present in control (i.e., untreated Cu₂O) and in 10 µg ml⁻¹. It means there was very little effect observed at 10 µg ml⁻¹ of Cu₂O-HMs concentration, but log phase was much delayed at the concentration of 50 and 80 µg ml⁻¹. At 110 µg ml⁻¹ of Cu₂O-HMs concentration, the log phase was completely absent.

Mechanism

There is very little study and still no clear-cut antibacterial mechanism of CuO-HMs has been proposed but possible mechanism of action of Cu ion and CuO-HMs has been suggested according to chemical, structural and morphological changes found in bacteria. Growth of pathogenic bacteria, *S. aureus* was completely checked at the 120 µg ml⁻¹ concentration of Cu₂O-HMs which shows efficient antibacterial properties due to their extremely large surface area which provide better adherence of CuO-HMs to bacterial cell membrane, as well as ROS generation on particle surface cause an increase of cell permeability, responsible to uncontrolled transport of CuO-HMs through the cytoplasmic membrane and consequently cell death. The antibacterial properties depend on the shape and size of CuO-HMs. The gram positive bacteria *S. aureus* cell wall is thick, consisting of large amount of mucopeptides as well as surface components of lipoteichoic acid (LTA) which make more resistant than *E. coli* against CuO-HMs [41].

Conclusion

In this study, we report the use of root carrot pulp waste as a reducing agent and capping agent responsible to synthesis Cu₂O-HMs. The important thing is the dry carrot pulp waste can be storable for future use and focus for maximum utilization of resources. CPWE mediated Cu₂O-HMs obtained pure phase and good particle morphology. This novel synthesis low cost, green and eco-friendly in compare conventional chemical reduction method. The FTIR analysis of Cu₂O-HMs powder shows the capping of the biomolecules on the surface of the CPWE mediated Cu₂O-HMs. Cu₂O-HMs surface modification may be biocompatible for biomedical applications and as a nano-coating for surgical devices and wound healing bandage.

Acknowledgements

Mr. Abhishek K. Bhardwaj is grateful to Central University of Allahabad, Allahabad UGC fellowship during D. Phil. We are also thankful to K.K. Pandey of RRCAT Indore and AIIMS for measurement of XRD and TEM, respectively.

References

1. Prabhu, S.; Poulouse, E. K.; *Int. Nano Lett.* **2012**, 2, 1. DOI: [10.1186/2228-5326-2-32](https://doi.org/10.1186/2228-5326-2-32)
2. Virkutyte, J.; Varma, R.S.; *Chem. Sci.*, **2011**, 2, 837. DOI: [10.1039/C0SC00338G](https://doi.org/10.1039/C0SC00338G)
3. Pandey, J. K.; Swarnkar R. K.; Soumya, K. K.; Dwivedi, P.; Singh, M. K.; Sundaram, S.; Gopal, R.; *Appl. Biochem. Biotechnol.*, **2014**, 174, 1021. DOI: [10.1007/s12010-014-0934-y](https://doi.org/10.1007/s12010-014-0934-y)
4. Zhang, H.; Zhu, Q.; Zhang, Y.; Wang, Y.; Zhao, Li.; Yu, B.; *Adv. Funct. Mater.*, **2007**, 17, 2766. DOI: [10.1002/adfm.200601146](https://doi.org/10.1002/adfm.200601146)
5. White, B.; Yin, M.; Hall, A.; Le, D.; Stolbov, S.; Rahman, T.; Turro, N.; O'Brien, S.; *Nano Lett.*, **2006**, 6, 2095. DOI: [10.1021/nl061457v](https://doi.org/10.1021/nl061457v)
6. Kuo, C. H.; Huang, M. H.; *J. Phys. Chem. C*, **2008**, 112, 18355. DOI: [10.1021/jp8060027](https://doi.org/10.1021/jp8060027)
7. Ho, J. Y.; Huang, M. H.; *J. Phys. Chem. C*, **2009**, 113, 14159. DOI: [10.1021/jp903928p](https://doi.org/10.1021/jp903928p)
8. Kuo, C. H.; Chen, C. H.; Huang, M. H.; *Adv. Funct. Mater.*, **2007**, 17, 3773. DOI: [10.1002/adfm.200700356](https://doi.org/10.1002/adfm.200700356)
9. Xu, H.; Wang, W.; Zhu, W.; *J. Phys. Chem. B*, **2006**, 110, 13829. DOI: [10.1021/jp061934y](https://doi.org/10.1021/jp061934y)
10. Yu, H.; Yu, J.; Liu, S.; Mann, S.; *Chem. Mater.*, **2007**, 19, 4327. DOI: [10.1021/cm070386d](https://doi.org/10.1021/cm070386d)
11. Hara, M.; Kondo, T.; Komoda, M.; Ikeda, S.; Kondo, J. N.; Domen, K.; Hara, M.; Shinohara, K.; Tanaka, A.; *Chem. Commun.*, **1998**, 29, 357. DOI: [10.1039/A707440I](https://doi.org/10.1039/A707440I)
12. Tang, B. X.; Wang, F.; Li, J. H.; Xie, Y. X.; Zhang, M. B.; *J. Org. Chem.*, **2007**, 72, 6294. DOI: [10.1021/jo070538o](https://doi.org/10.1021/jo070538o)
13. McShane, C. M.; Choi, K. S.; *J. Am. Chem. Soc.*, **2009**, 131, 2561. DOI: [10.1021/ja806370s](https://doi.org/10.1021/ja806370s)
14. Yang, Z.; Chiang, C. K.; Chang, H. T.; *Nanotech.*, **2008**, 16, 025604. DOI: [10.1088/0957-4484/19/02/025604](https://doi.org/10.1088/0957-4484/19/02/025604)
15. Fan, W. Y.; Ng, C. H.; *J. Phys. Chem. B*, **2006**, 110, 20801. DOI: [10.1021/jp061835k](https://doi.org/10.1021/jp061835k)
16. Pugazhendhi, S.; Kirubhaa, E.; Palanisamy, P. K.; Gopalakrishnan; *Appl. Surf. Sci.*, **2015**, 357, 1801. DOI: [10.1016/j.apsusc.2015.09.237](https://doi.org/10.1016/j.apsusc.2015.09.237)
17. de Jongh, P. E.; Vanmaekelbergh, D.; Kelly, J. J.; *Chem. Mater.*, **1999**, 11, 3512. DOI: [10.1021/cm991054e](https://doi.org/10.1021/cm991054e)
18. Huang, L. N.; Wang, H. T.; Wang, Z. B.; Mitra, A.; *Chem. Mater.*, **2002**, 14, 876. DOI: [10.1021/cm010819r](https://doi.org/10.1021/cm010819r)
19. Barton, J. K.; Vertegel, A. A.; Bohannon, E. W.; *Chem. Mater.*, **2001**, 13, 952. DOI: [10.1021/cm000707k](https://doi.org/10.1021/cm000707k)
20. Dhas, N. A.; Raj, C. P.; Gedanken, A.; *Chem. Mater.* **1998**, 10, 1446. DOI: [10.1021/cm9708269](https://doi.org/10.1021/cm9708269)
21. Deki, S.; Akamatsu, K.; Yano, T.; Mizuhata, M.; Kajinami, A.; *J. Mater. Chem.*, **1998**, 8, 1865. DOI: [10.1039/A801506F](https://doi.org/10.1039/A801506F)
22. Wang, W.; Wang, G.; Wang, X.; Zhan, Y.; Liu, Y.; *Adv. Mater.*, **2002**, 14, 67. DOI: [10.1002/1521-4095\(20020104\)14:1<67::AID-ADMA67>3.0.CO;2-Z](https://doi.org/10.1002/1521-4095(20020104)14:1<67::AID-ADMA67>3.0.CO;2-Z)
23. Yanagimoto, H.; Akamatsu, K.; Gotoh, K.; Deki, S.; *J. Mater. Chem.*, **2001**, 11, 2387. DOI: [10.1039/B102444M](https://doi.org/10.1039/B102444M)
24. Swarnkar, R. K.; Gopal, R.; *Sci. Adv. Mater.*, **2012**, 511. DOI: [10.1166/sam.2012.1311](https://doi.org/10.1166/sam.2012.1311)

25. Shukla, A.; Singh, S. C.; Pandey, B. K.; Uttam, K. N.; Shah, J.; Kotnala R. K.; Gopal, R.; *Adv. Mater. Lett.*, **2015**, *6*, 1066.
DOI: [10.5185/amlett.2015.5930](https://doi.org/10.5185/amlett.2015.5930)
26. Tang, S. L. Y.; Smith, R. L.; Poliakov, M.; *Green Chem.*, **2005**, *7*, 761.
DOI: [10.1039/B513020B](https://doi.org/10.1039/B513020B)
27. Poliakov, M.; Anastas, P.; *Nature*, **2001**, *413*, 257–257.
DOI: [10.1038/35095133](https://doi.org/10.1038/35095133)
28. Iravani, S., *Green Chem.*, **2011**, *13*, 2638.
DOI: [10.1039/C1GC15386B](https://doi.org/10.1039/C1GC15386B)
29. Luque, R., Varma, R. S. (Eds); Sustainable Preparation of Metal Nanoparticles: Methods and Applications; Royal Society Chemistry: UK, **2012**.
DOI: [10.1039/9781849735469](https://doi.org/10.1039/9781849735469)
30. Ruparelia, J. P.; Chatterjee, A. K.; Duttagupta, S. P.; Mukherji, S.; *Acta Biomater.* **2008**, *4*, 707.
DOI: [10.1016/j.actbio.2007.11.006](https://doi.org/10.1016/j.actbio.2007.11.006)
31. Wei, Y.; Chen, S.; Kowalczyk, B.; Huda, S.; Gray, T.P.; Grzybowski, B.A.; *J Phys Chem C.* **2010**, *114*, 15612.
DOI: [10.1021/jp1055683](https://doi.org/10.1021/jp1055683)
32. Zain, N. M.; Stapley, A. G. F.; Shamaa, G.; *Carbohydr. Polym.*, **2014**, *112*, 195.
DOI: [10.1016/j.carbpol.2014.05.081](https://doi.org/10.1016/j.carbpol.2014.05.081)
33. Umadevi, M.; Shalini, S. Bindhu, M. R.; *Adv. Nat. Sci.: Nanosci. Nanotechnol.*, **2012**, *03*, 025008.
DOI: [10.1088/2043-6262/3/2/025008](https://doi.org/10.1088/2043-6262/3/2/025008)
34. Xiong, J.; Wang, Y.; Xue, Q.; Wu, X.; *Green Chem.*, **2011**, *13*, 1900.
DOI: [10.1039/C0GC00772B](https://doi.org/10.1039/C0GC00772B)
35. Swarnkar, R. K.; Singh, S. C.; Gopal, R.; *Bull. Mater. Sci.*, **2011**, *34*, 1363.
DOI: [10.1007/s12034-011-0329-4](https://doi.org/10.1007/s12034-011-0329-4)
36. Dang, T. M. D.; Le, T. T.; Fribourg-Blanc, E.; Dang, M. C.; *Adv. Nat. Sci.: Nanosci. Nanotechnol.* **2011**, *2*, 015009.
DOI: [10.1002/sml.201200772](https://doi.org/10.1002/sml.201200772). Epub 2012 Aug 13.
37. Silva, F. A. M.; Borges, F.; Guimaraes, C.; Lima, J. L. F. C.; Matos, C.; Reis, S.; *J Agric Food Chem.*, **2000**, *48*, 2122.
DOI: [10.1021/jf9913110](https://doi.org/10.1021/jf9913110)
38. Singh, S. C.; Gopal, R.; *Appl. Surf. Sci.*, **2012**, *258*, 2211.
DOI: [10.1016/j.apsusc.2011.05.018](https://doi.org/10.1016/j.apsusc.2011.05.018)
39. Kliche, G.; Popovic, Z. V.; *Phys. Rev.*, **1990**, *42*, 10060.
DOI: [10.1103/PhysRevB.42.10060](https://doi.org/10.1103/PhysRevB.42.10060)
40. Titirici, M. M.; Antonietti, M.; Thomas, A.; *Chem. Mater.*, **2006**, *18*, 3808.
DOI: [10.1021/cm052768u](https://doi.org/10.1021/cm052768u)
41. Applerot, G.; Lellouche, J.; Lipovsky, A.; Nitzan, Y.; Lubart, R.; Gedanken, A.; Banin, E.; *Small*, **2012**, *21*, 3326.
DOI: [10.1002/sml.201200772](https://doi.org/10.1002/sml.201200772). Epub 2012 Aug 13